Energy Conversion and Management 319 (2024) 118915

Contents lists available at ScienceDirect

Energy Conversion and Management

journal homepage: www.elsevier.com/locate/enconman

Research Paper

Modelling and optimization of concentrated solar power using response surface methodology: A comparative study of air, water, and hybrid cooling techniques

Ayman Mdallal [a], Salah Haridy [a,b,c], Montaser Mahmoud [a], Abdul Hai Alami [a], Abdul Ghani Olabi [a,*], Mohammad Ali Abdelkareem [a,d]

[a] Sustainable Energy & Power Systems Research Centre, RISE, University of Sharjah, P.O. Box 27272, Sharjah, United Arab Emirates
[b] Department of Industrial Engineering and Engineering Management, College of Engineering, University of Sharjah, Sharjah, United Arab Emirates
[c] Benha Faculty of Engineering, Benha University, Benha, Egypt
[d] Chemical Engineering Department, Minia University, Elminia, Egypt

ARTICLE INFO

Keywords:
Concentrated Solar Power
Parabolic trough collector
Response Surface Methodology
Optimization

ABSTRACT

This research introduces a novel approach specifically designed to improve the design of Concentrated Solar Power plants utilizing the Response Surface Methodology. The objective of the suggested methodology is to enhance energy production efficiency by simultaneously minimizing the levelized cost of electricity and the land footprint associated with the power plant while comparing three different cooling techniques: air, water, and hybrid. Two software tools, System Advisor Model and Design-Expert, are employed to validate the primary model, evaluate the responses, generate the predictive models, and verify the results. The configuration of a Concentrated Solar Power plant is influenced by four main factors: the size of the solar field (solar multiple), row spacing, number of solar assemblies per loop, and size of thermal energy storage. In this study, these factors are varied within the following ranges: solar multiple from 1 to 5, row spacing from 10 to 30 m, number of solar assemblies from 4 to 10 per loop, and thermal energy storage from 5 to 15 h. The generated predictive models demonstrated very high accuracy, particularly for the annual energy production, with an error ranging between 0.2% and 1.5%. The findings showed that the hybrid cooling system is the most cost-effective cooling technique and has the highest energy output compared to the evaporative and air-cooling methods. When optimizing the required area of the hybrid cooled plant with a reduction of 47.44%, the analysis indicated a minimal decrease in energy output of 3.61% and a slight increase in the levelized cost of electricity by 0.95%. According to the results, the effect of area on the annual energy production and levelized cost of electricity is significant below the optimal area, while this effect becomes minor at higher values.

1. Introduction

Concentrated Solar Power (CSP) is a promising renewable energy technology that uses sunlight to produce electricity. CSP systems concentrate sunlight onto a central receiver to generate high-temperature heat [1], unlike PV systems that turn sunlight into electricity using semiconductor materials [2]. Then, this heat is utilized to power turbines and produce energy. CSP has benefits such as energy storage capacity and the ability to generate electricity even in the absence of sunlight.

According to the International Energy Agency (IEA), worldwide demand for electricity increased slightly in 2023 but is expected to accelerate through 2026. While developed nations faced declines due to adverse macroeconomic conditions and inflation, electricity demand in China, India, and several Southeast Asian countries increased significantly. Over the next three years, global electricity demand is predicted to rise at an annual rate of 3.4 %. By early 2025, renewables are expected to account for more than one-third of total global electricity output, surpassing coal. Renewables are expected to increase their share of energy generation from 30 % in 2023 to 37 % in 2026, due to the spread of increasingly affordable solar photovoltaic technology. China's electricity demand increased by 6.4 % in 2023, with the services and

* Corresponding author.
E-mail address: aolabi@sharjah.ac.ae (A.G. Olabi).

https://doi.org/10.1016/j.enconman.2024.118915
Received 29 March 2024; Received in revised form 9 July 2024; Accepted 8 August 2024
Available online 15 August 2024

Table 1
Summary of optimization studies on Concentrated Solar Power.

Reference	Technology	Method	Optimization/ Objective
Zayed et al. [13]	Dish/Stirling CSP	Multi-Objective Particle Swarm Optimization	Maximize the output power and total efficiency
Li et al. [14]	CSP hybridized with combined heat plant	three-stage multi-time scale stochastic unit commitment-economic dispatch model	Maximize energy utilization efficiency
Jiang et al. [15]	CSP hybridized with Wind turbine, combined heat plant and electric energy storage	Integrated Demand Response	Maximize operating efficiency and minimize cost
Hamilton et al. [16]	Solar Thermal Tower CSP hybridized with PV plant	System Advisor Model (SAM) Simulation Core	Maximize plant revenue
Elbeh and Sleiti [17]	Solar Thermal Tower CSP	SolarPILOT and SAM	Maximize Energy Production
Ma et al. [18]	Solar Thermal Tower CSP with S-CO_2 cycle	MATLAB 2018a platform	Minimize the levelized cost of electricity (LCOE)
Liang et al. [19]	Solar Thermal Tower CSP with S-CO_2 cycle and Organic Rankine Cycle	nonlinear programming model	Enhance Thermal Efficiency
Trevisan et al. [20]	Solar Thermal Tower CSP with S-CO_2 cycle	Quasi Steady State Thermo-Economic Model (MATLAB R2019b)	Minimize the LCOE and increase the capacity factor
Ahmad and Zeeshan [21]	Solar Thermal Tower and parabolic trough collector CSP plants	Tailored algorithm	Minimize the LCOE and environmental impact avoided
Cox et al. [22]	Solar Thermal Tower	AMPL modeling language and Gurobi	Maximize plant revenue
Wang et al. [23]	Solar Thermal Tower	the improved IEEE 30-bus system	Minimize system operation costs

industrial sectors driving the growth. Although the rate of development is likely to slow, China's total rise in electricity demand through 2026 is significant (roughly 1,400 TWh), or more than half of the European Union's present annual electricity consumption. Data centers, artificial intelligence (AI), and the cryptocurrency sector are major drivers of global electricity demand growth, with consumption potentially doubling by 2026 [3]. According to the International Renewable Energy Agency (IRENA), the cumulative installed capacity of renewable energy systems by 2023 was 3.87 TW worldwide, more than 50 % were installed in Asia alone. Around 36.7 % (1.42 TW) of the installed systems were solar energy systems, with photovoltaics making the highest contribution by 36.5 % (1.412 TW) and only 0.2 % (about 7 GW) for CSP plants [4].

CSP systems use mirrors or lenses to focus sunlight onto a receiver [5] and there are four main different technologies including, solar tower, linear Fresnel, Parabolic Trough, and Dish Sterling [6]. A working fluid, such as heat transfer oil or molten salt, absorbs the concentrated solar energy and heats up. The fluid is heated and passes its energy to a heat exchanger, creating steam that powers turbines connected to generators, resulting in the production of electricity. The essential elements of a CSP system consist of solar collectors that concentrate sunlight onto the receiver, the receiver where the working fluid absorbs solar energy, the heat exchanger that transfers heat from the working fluid to generate steam, and turbines and generators that transform steam energy into electricity. CSP technology provides benefits such as energy storage for generating electricity after sunset, the option to combine with fossil fuels or other renewables for continuous power supply [7], and suitability for desert environments with abundant direct solar radiation, making arid deserts ideal for CSP plants but the soiling effect in that case is considered to be a major challenge [8]. CSP cooling systems are available in three types, each exhibiting its own advantages and disadvantages. Air-cooled systems do not consume water or require water treatment and have lower operation and maintenance costs, but they have higher equipment costs, more expensive load handling, and higher parasitic energy costs. Evaporative cooling systems have the lowest installation cost, best cooling efficiency at low temperatures, especially in arid climates, and highest power cycle efficiency, but they require significant amount of water, essential water treatment, and higher maintenance due to cold weather plume in the cooling tower. Hybrid cooling systems reduce water consumption, lower cooling energy costs during mixed dry/wet periods, and maintain good performance in hot weather, but they can have high capital costs and disadvantages that vary with design and climate [9]. There are currently about 154 CSP projects in the world, of which 116 are operational, 20 are decommissioned or non-operational, and 18 are being built with plans to start soon [10]. Based on the comparison, China, Spain, and the US are the top three countries using CSP plants. The largest installed capacity is in Spain, at 2.3 GW, from 51 fully operational projects spread across the country. Out of the four popular CSP technologies, parabolic trough collectors (PTC) are the most widely used, with 91 projects. Solar thermal towers come in second with 34 projects, followed by linear Fresnel reflectors with 16 projects, and there are just two dish projects, both of which are decommissioned. The PTC technology was employed in about 75 % of the installed capacity [9].

There are various obstacles preventing CSP from being widely used. High investment costs are a major obstacle due to the complex infrastructure required for concentrating sunlight, capturing heat, and producing power [11]. Additionally, CSP systems require significant water use for diverse activities, which might be limiting, particularly in desert areas [12]. The large land area required for CSP facilities, which must house mirrors or heliostats, presents difficulties in land acquisition, especially in densely populated regions. Additionally, the market penetration of CSP is slowed by competition from more cost-effective PV, which has lower overall capital costs and are preferred by investors and stakeholders. Finally, the complex design of CSP systems, which includes components such as mirrors and heat transfer fluids, requires extremely organized maintenance, leading to increased operational challenges and costs [11]. In recent years, several studies have explored various methods for multi-objective optimization in CSP plants. These optimization efforts aim to achieve higher energy output, cost reduction, or a combination of both. Researchers have investigated different parameters that significantly impact CSP plant performance, as summarized in Table 1.

Response Surface Methodology (RSM) is an effective method employed to optimize responses in cases involving two or more quantitative parameters. In this approach, the variables that are influenced by other factors are called responses, while the variables that have an impact on the responses are usually known as predictor variables. The goal of RSM is to identify the optimal combination of continuous factor levels that either maximize or minimize the desired outcome. RSM utilizes the analysis of overlapping descriptors and their similarities to determine the optimal conditions for obtaining the best outcomes in different experiments [24]. The main components of RSM include factor variables, which are the independent variables or factors that have an influence on the response; and response variables, which are the dependent variables (or responses) that we seek to optimize. RSM is an experimental design approach that involves evaluating the statistical significance of the factor variables. In addition, a regression model, often a second-degree polynomial, is created to explain the correlation between variables and the outcome. This is then followed by optimization, which aims to identify the factor levels that maximize or minimize the outcome based on the fitted model. RSM is utilized in many fields such as industrial, manufacturing, medical sciences, and engineering

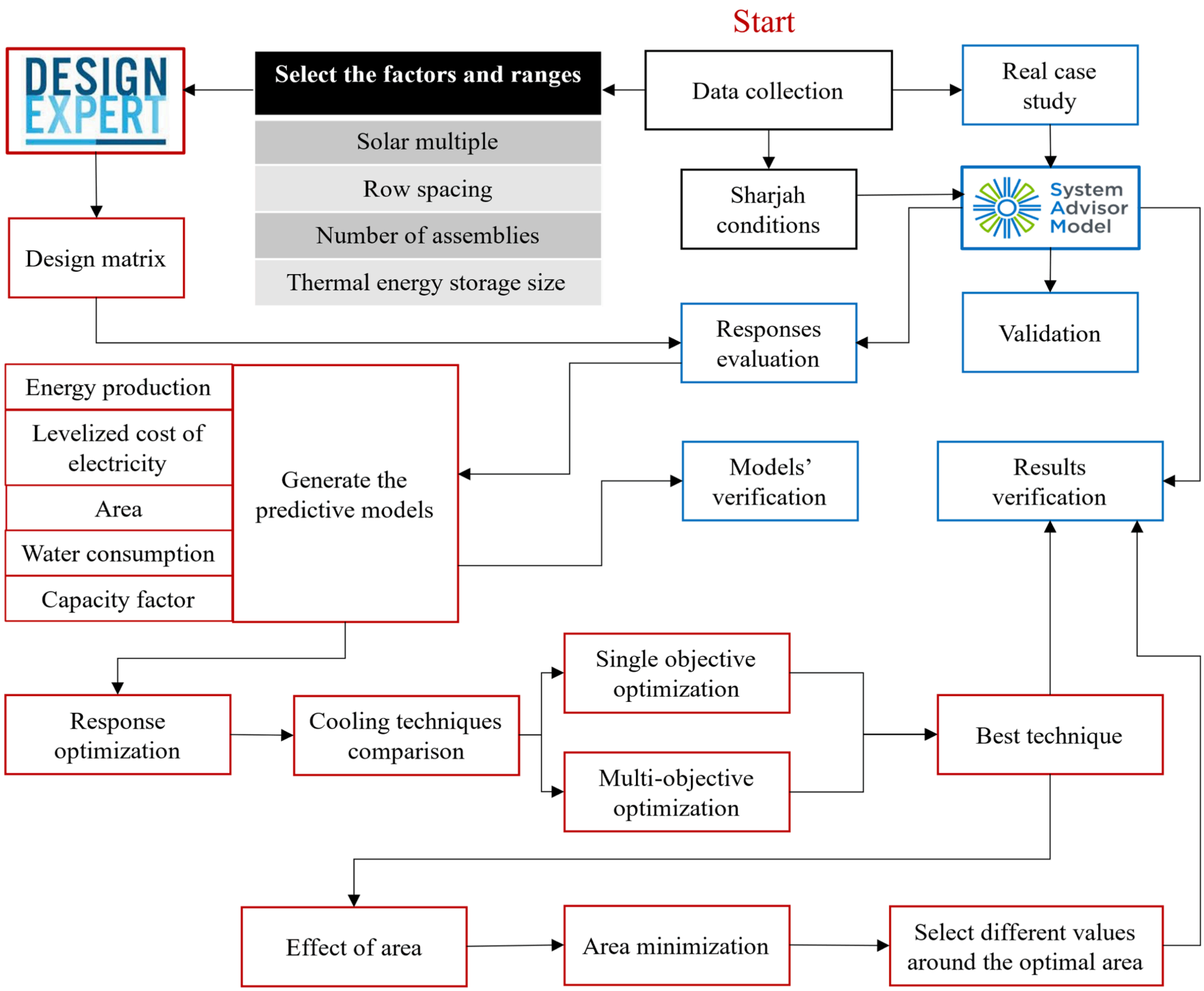

Fig. 1. Research flow chart. The red color refers to the steps related to Design-Expert and the blue color refers to those of SAM.

research [25]. RSM offers several advantages and has some limitations. On the advantages side, RSM allows for the optimization of experimental conditions by analyzing the response of multiple variables simultaneously, helping to efficiently find the best combination of factors to achieve the desired outcome. Additionally, RSM provides a regression model that estimates the behavior of the system, enabling efficient decision-making and resource allocation [26].

RSM has been employed in multiple investigations to simulate and enhance a solar-powered renewable energy system including hot water, cooling, and electricity generation. An assessment was conducted in Australia to determine the feasibility of a photovoltaic thermal (PV/T) technology system [27]. Local climatic data was used for this evaluation, and optimization was conducted by employing RSM and the Engineering Equation Solver (EES). The system was improved in two scenarios to reduce costs and improve exergy efficiency. As a result, it achieved an exergy efficiency of 19.704 % and a cost rate of 1.774 $/h. A cost analysis revealed that the organic Rankine cycle (ORC) and proton exchange membrane (PEM) electrolyzer have expensive operational expenses. Additionally, there is a substantial loss of energy in many subsystems, resulting in significant exergy destruction. In another research, a statistical model utilizing RSM and COMSOL 5.4 Multiphysics software accurately predicted the electrical efficiency of a concentrated photovoltaic-thermoelectric (CPV-TE) system, with a determination coefficient (R^2) of 0.99. The study further examined the influence of factors such as solar radiation, optical concentration, and ambient temperature on efficiency, resulting in a maximum efficiency of 17.448 % [28]. Utilizing RSM combined with PVsyst, Radwan et al. [29] conducted a comprehensive investigation of the parameters affecting the annual energy generation of tilted bifacial PV systems in Sharjah, UAE. The study determined that optimizing the module spacing, tilt angle, and ground albedo has a major beneficial impact on energy production.

As presented in the literature, RSM has shown great potential as an optimization method and especially when multi-objective optimization is required. Additionally, it has proven to be an effective tool for investigating the statistical significance of the input factors on the responses and optimizing solar energy systems. In this context, a novel approach specifically designed for optimizing CSP plants using RSM is introduced in the current study. The methodology focuses on maximizing energy output while minimizing both the levelized cost of electricity (LCOE) and the land area required for the power plant considering three different cooling techniques (air, evaporative, and hybrid). Four critical factors that influence CSP plant design including solar field size (solar multiple), row spacing, thermal energy storage size, and number of solar assemblies per loop are considered. RSM is also utilized to develop a regression model representing the annual energy generation and LCOE of a proposed CSP system design in terms of these input factors. By integrating RSM into our optimization framework, we

Table 2
Andasol 1 validation results.

Parameter	Reported Value [34]	SAM Result	Error (%)
Annual Energy (kWh)	179,103,000	174,738,960	2.44 %
Capacity factor (%)	41.50	39.9	3.86 %
PPA price (¢/kWh)	37.05	37.32	0.73 %
Total Installed Cost ($)	411,690,000	409,743,371.35	0.47 %
Total Land Area (Acres)	481.85	480	0.38 %

Table 3
Andasol 1 Performance results in Sharjah compared to the original location using SAM.

Parameter	Granada (Evaporative)	Sharjah (Evaporative)	Sharjah (Air)	Sharjah (Hybrid)
Annual Energy (kWh)	174,738,960	162,879,072	160,962,080	162,171,168
Capacity factor (%)	39.9	37.2	36.7	37
LCOE (¢/kWh)	21.16	22.24	22.36	22.26
Water Usage (m^3)	588,218	599,769	38,582	318,452
Total Area (Acres)	480			

aim to achieve an optimal CSP plant configuration that balances energy production, cost-effectiveness, and land utilization. Our findings contribute to advancing sustainable and economically viable solar energy solutions.

2. Methods

This study employs two software tools, namely System Advisor Model (SAM) [30] and Design-Expert [31]. An illustration of the steps followed in this research is depicted in Fig. 1, which highlights the role of each software tool in optimizing the three key performance indicators. SAM software is mainly used for three purposes: primary model validation, responses evaluation, and results verification.

First, the data is collected considering a real case study that is discussed in detail in the next section. The same conditions of the real application are applied to the simulations carried out through SAM to validate the primary model. Meanwhile, four different effective parameters are investigated: solar multiple, row spacing, number of assemblies per loop, and thermal energy storage size. For each of these factors, a range is identified in order to generate the design matrix through Design-Expert. This matrix is then entered as an input to the validated SAM model to evaluate the required responses (energy production, capacity factor, area, water consumption, and LCOE). These responses are used to generate predictive models utilizing Design-Expert, which are used to implement the optimization procedures.

The first stage of optimization is conducted to select the best cooling method among air, evaporative, and hybrid cooled (50 % air-cooled and 50 % evaporative). The best method is chosen based on two optimization approaches: single-objective and multi-objective. In the single-objective optimization, the energy is maximized and LCOE is minimized (each alone). However, in the multi-objective approach, both are optimized. After selecting the best cooling method, the optimal value of the area is determined considering three objectives (maximizing energy, minimizing LCOE, and minimizing area). Finally, different values of area are taken as constraints (around the optimal area) to investigate the influence of the area on the energy output and LCOE considering the best cooling method. In all optimization stages, the results of the predicted responses are verified using the validated model.

2.1. Simulation and validation

Andasol 1 is the first CSP plant in Europe to use Parabolic Trough Collector (PTC) technology. The plant is located in Granada, southern Spain, at coordinates 37° 13′ 42.7″ N, 3° 4′ 6.73″ W. It covers about 481.85 acres (1 acre = 4046.86 m^2) and produces up to 180 GWh of energy annually. The EuroTrough (ET150) operates as a solar collector technology with a total reflective surface area of 510,120 m^2. The collectors are oriented on the North-South axis and have East-West solar tracking systems, which are enabled by separate solar sensors for accurate sun tracking. The solar field uses Dowtherm A as the heat transfer medium, specifically designed for high-temperature purposes up to 400 °C. This is crucial for effective heat collecting, transportation, and storage in CSP systems. Andasol's significant feature is its use of a molten salt thermal storage system, which includes a salt mixture of 60 % sodium nitrate ($NaNO_3$) and 40 % potassium nitrate (KNO_3). This mixture has a melting point of 227 °C and a vaporization threshold of 600 °C. The storage tanks are 14 m tall and have a diameter of 36 m. It has a capacity of 1 GWh, which is enough to keep the turbine running for about 7.5 h, as described in Equation (1). Andasol 1 utilizes a steam Rankine cycle to generate power, with a turbine capacity of 55 MW and a wet cooling system [32]. The thermal energy storage (TES) thermal capacity (C) or the storage hours at the design point ($t_{full\ load}$) can be estimated as follows:

$$C = \frac{\dot{W}_{des.gross}}{\mu_{des}} * t_{fullload} \tag{1}$$

$$t_{fullload} = \frac{C * \mu_{des}}{\dot{W}_{des.gross}} = \frac{1000MWh * 0.381}{50MW} \cong 7.5h$$

where $\dot{W}_{des.gross}$ is the design turbine gross output and μ_{des} is the cycle thermal efficiency.

This power plant is used as a reference in this study to construct a model and perform a simulation, using System Advisor Model (SAM) v2023.12.17 developed by the National Renewable Energy Laboratory (NREL). The simulated model is then used to validate the results with the real results. After that, the simulation is conducted in Sharjah, UAE. The hourly meteorological data files for both Granada and Sharjah are obtained through the National Solar Radiation Database (NSRDB) [33]. In order to build the reference model, all data, input parameters, and reported values are obtained from "System Advisor Model (SAM) Case Study: Andasol-1" [34]. The same design parameters are applied to the simulations considering the new location (Sharjah). Only the weather data is changed based on the location. The validation results of our model are shown in Table 2.

The slight difference (2.44 %) in the energy output between the SAM model and the reported value from the case study can be attributed to factors such as weather data accuracy and heat loss. Accurate solar irradiance, ambient temperature, and wind speed data are crucial, as inconsistency may arise if the weather data does not match real-world conditions. Additionally, heat losses during energy conversion, such as in the Rankine cycle, affect overall efficiency. All validated parameters showed a high level of accuracy with an error of less than 5 %. The LCOE is not included in the validation due to the insufficient financial input parameters obtained from the case study, which are required to get an accurate estimate of the LCOE. This is also attributed to the rapid development of the technology in the past 11 years that resulted in a massive reduction in the LCOE of this technology which is also reflected in SAM software between v2012 and v2023.

After the validation, the weather data file is changed for Sharjah, UAE and the results obtained are shown in Table 3. These results are used as a benchmark in order to conduct a comparison between three different cooling methods (evaporative, air, and hybrid cooling systems). Subsequently, a multi-objective optimization is conducted to improve the energy output and reduce the LCOE and total land area

Table 4
Input parameters and their levels.

Parameter	Levels	
	Low	**High**
A: Solar multiple	1	5
B: Row spacing (m)	10	30
C: No. of solar collector assemblies per loop	4	10
D: Thermal energy storage size (h)	5	15

required for this plant for the best selected cooling method.

2.2. Response Surface Methodology

Response Surface Methodology (RSM) is an effective approach used to improve system performance by analyzing several design aspects [35]. It can offer a statistical model that can estimate the annual energy yield, LCOE, and total land area of the system. This estimation considers the design factors and their interactions. When dealing with scenarios where multiple factors influence a desired outcome and the objective is to optimize this outcome, RSM offers a variety of valuable statistical and mathematical techniques. It enables the effective examination and improvement of system efficiency [29]. The RSM employs a second-order polynomial equation to establish a relationship between the response variable y and a set of N design factors [36,37]. This relationship is represented by Equation (2) as follows:

$$y = \beta_0 + \sum_{i=1}^{N}\beta_i x_i + \sum_{i=1}^{N}\beta_{ii}{x_i}^2 + \sum_{i=1}^{N-1}\sum_{j>i}^{N}\beta_{ij}x_i x_j + \epsilon \quad (2)$$

Consider a scenario where we have a response variable of interest denoted by y and a set of input parameters represented by x_i. The response variable y's observed error is denoted by the term ϵ. Additionally, N represents the total number of parameters. The coefficients involved in our model are as follows:

- β_0: the free coefficient.
- β_i: the linear coefficient.
- β_{ii}: the quadratic coefficient.
- β_{ij}: the interaction coefficient.

In order to minimize the sum of squared errors, the coefficients are estimated utilizing the ordinary least squares (OLS) approach. Table 4 presents a full list of the input parameters that necessitate optimization. The RSM analysis employs two levels for each parameter.

- Solar multiple: the ratio of the thermal power generated by the solar field under design conditions to the thermal power needed by the power block under nominal conditions.
- Number of solar collector assemblies per loop: the solar collector assemblies are a group of adjacent collectors operated by a single drive. To reach the desired temperature in the heat transfer fluid, the assembly is replicated multiple times within a single loop.
- Row spacing: the center-to-center distance between the solar field loops.
- Thermal energy storage: used to store any excess thermal energy produced from the solar field, the size is primarily determined by the required thermal capacity from the solar field.

In this research, we employ RSM with a face-centered composite design [38], which includes three types of points:

1. Factorial Points: they are located at the corners of the design space and help estimate the linear and interaction effects.
2. Center Points: they are positioned at the center of the design space and provide information about the curvature of the response surface.
3. Axial Points: they are located on the faces of the design space and used to estimate quadratic terms.

Unlike the central composite design RSM, the face-centered composite design provides a balanced design by placing axial points at the

Table 5
Design matrix for the hybrid system.

Run No.	Input Parameters				Response(s)				
	A	B	C	D	Energy (kWh)	Capacity factor (%)	LCOE (¢/kWh)	Water consumption (m^3)	Area (Acres)
1	1	10	4	5	80,901,840	18.5	28.02	170,883	183
2	5	10	4	5	213,502,480	48.7	24.81	457,032	907
3	1	30	4	5	86,828,856	19.8	27.01	182,988	548
4	5	30	4	5	212,109,744	48.4	25.24	470,202	2721
5	1	10	10	5	72,318,936	16.5	29.98	163,059	185
6	5	10	10	5	216,170,432	49.4	24.71	457,562	908
7	1	30	10	5	79,653,408	18.2	28.37	177,969	554
8	5	30	10	5	228,318,656	52.1	24.14	481,062	2724
9	1	10	4	15	77,971,872	17.8	36.76	170,378	183
10	5	10	4	15	333,468,288	76.1	20.4	656,915	907
11	1	30	4	15	83,925,288	19.2	35.14	182,493	548
12	5	30	4	15	319,167,552	72.9	21.22	644,373	2721
13	1	10	10	15	69,414,704	15.8	40.81	162,994	185
14	5	10	10	15	339,091,392	77.4	20.14	681,640	908
15	1	30	10	15	76,591,784	17.5	37.3	177,942	554
16	5	30	10	15	344,158,976	78.6	20.19	691,931	2724
17	1	20	7	10	87,385,928	20	30.46	187,418	366
18	5	20	7	10	303,626,368	69.3	20.78	610,245	1817
19	3	10	7	10	244,371,072	55.8	20.25	478,649	546
20	3	30	7	10	259,963,408	59.4	19.65	507,318	1637
21	3	20	4	10	256,355,984	58.5	19.78	497,265	1091
22	3	20	10	10	248,066,240	56.6	20.14	495,255	1098
23	3	20	7	5	214,178,496	48.9	20.84	423,034	1091
24	3	20	7	15	276,967,136	63.2	20	535,398	1091
25	3	20	7	10	261,283,136	59.7	19.53	507,792	1091
26	3	20	7	10	261,283,136	59.7	19.53	507,792	1091
27	3	20	7	10	261,283,136	59.7	19.53	507,792	1091
28	3	20	7	10	261,283,136	59.7	19.53	507,792	1091
29	3	20	7	10	261,283,136	59.7	19.53	507,792	1091
30	3	20	7	10	261,283,136	59.7	19.53	507,792	1091

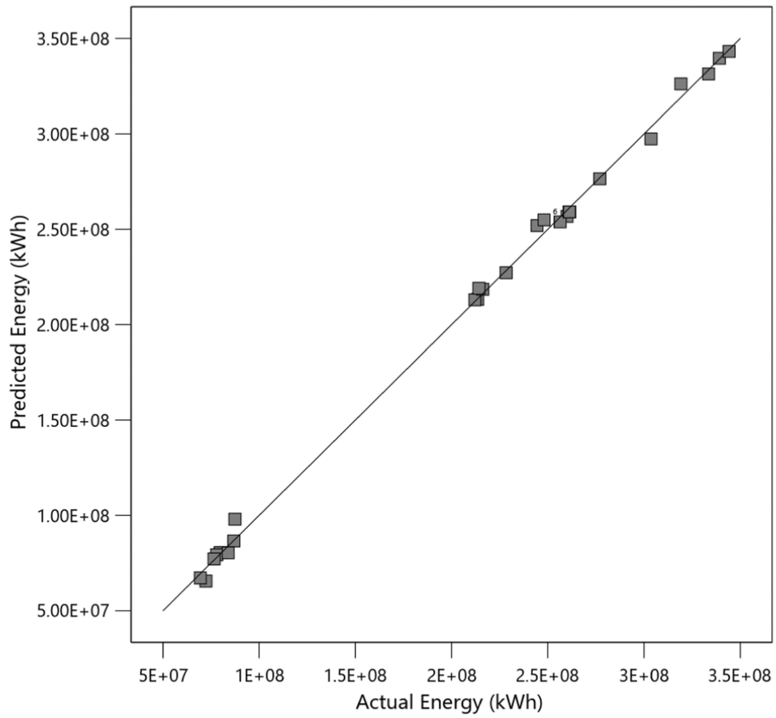

(a)

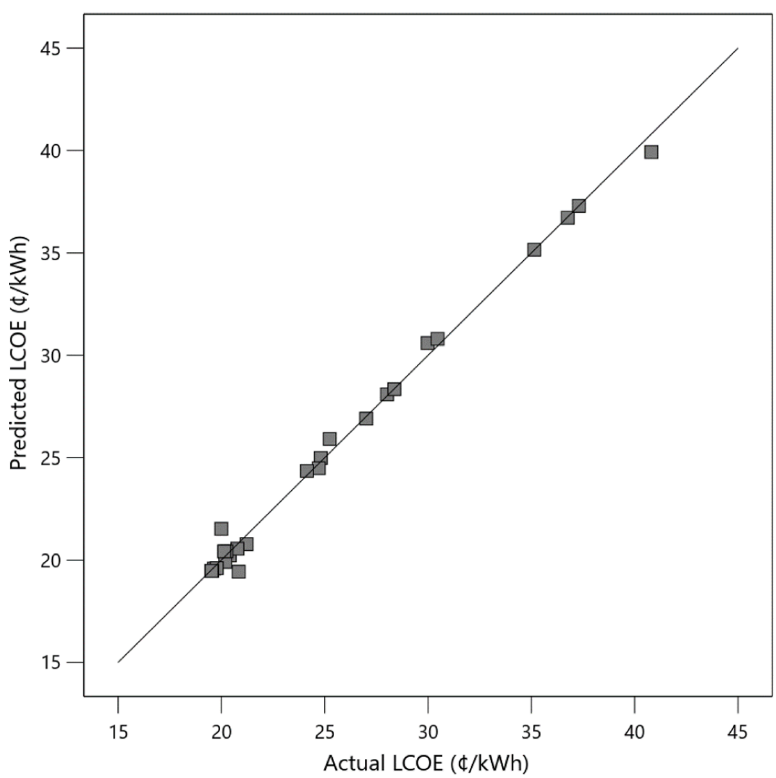

(b)

Fig. 2. The predicted vs. actual values of (a) annual energy and (b) LCOE.

center of the design faces. This avoids extreme or negative values and makes the experimental conditions more feasible and practical. It also allows for the assessment of both linear and interaction effects among the factors, leading to a more comprehensive understanding of the system. Finally, face-centered composite design is flexible and can be applied to various experimental conditions, making it suitable for optimizing complex processes like CSP plants.

Using this approach, a design matrix can be generated for each of the

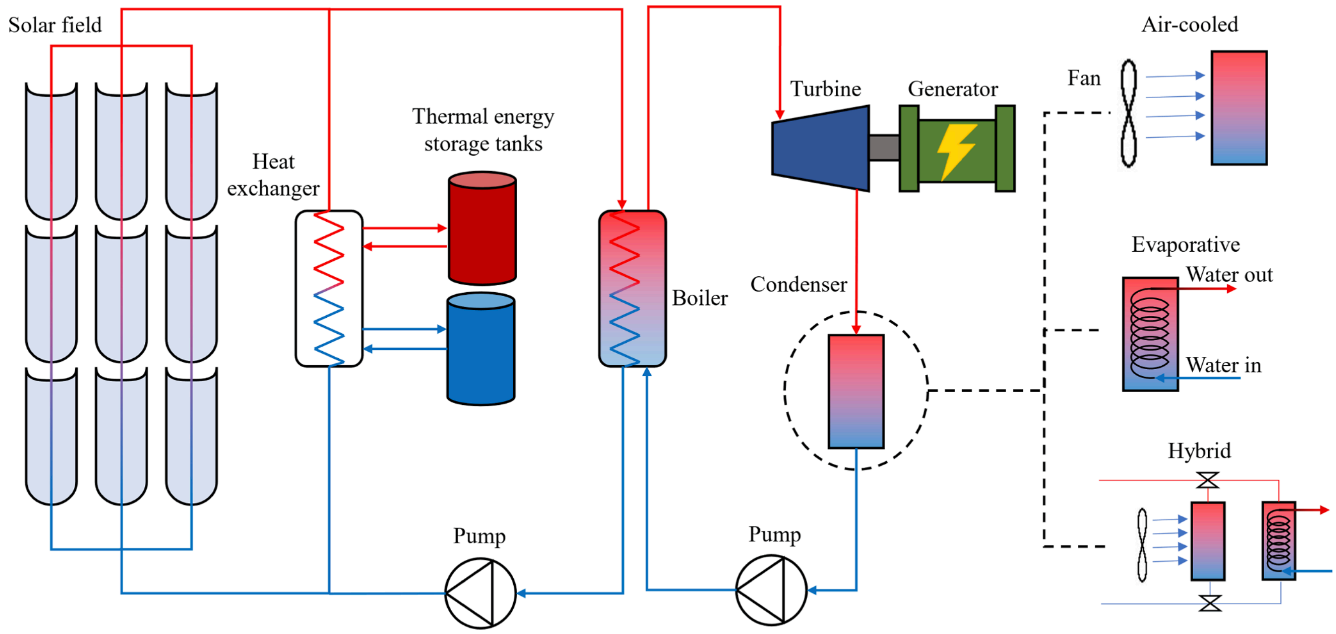

Fig. 3. Schematic diagram of the CSP, with three different cooling techniques configurations.

cooling methods. An example of a design matrix is presented in Table 5, showing the case of hybrid-cooled system and its responses using SAM. The coefficients (β_0, β_i, β_{ii}, and β_{ij}) of the polynomial equation are estimated using the resultant values in relation to each of the parameters. These coefficients contribute to our understanding of the system's behavior and guide optimization efforts [39].

2.3. Optimization method

To determine the optimal position and size of the step, the desirability optimization method has been employed. The method was established by Derringer and Suich [40]. This method is selected due to its effectiveness in determining the optimal values of the design factors that yield the desired responses simultaneously. This method operates based on the desirability function approach. Each response (y_i) is converted into an individual desirability function (d_i), ranging from 0 to 1, where one is the most favorable case and zero is the least favorable. The ultimate objective is to maximize the overall desirability (D), which is a combination of the individual desirability functions (d_i) associated with each response. If the objective or target T_i for the response y_i is a maximum value, then:

$$d_i = \begin{cases} 0 y_i < L_i \\ \left(\frac{y_i - L_i}{T_i - L_i}\right)^r L_i \le y_i \le T_i \\ 1 y_i > T_i \end{cases} \tag{3}$$

On the other hand, if the objective T_i for the response is a minimum value, then:

$$d_i = \begin{cases} 1 y_i < T_i \\ \left(\frac{U_i - y_i}{U_i - T_i}\right)^r T_i \le y_i \le U_i \\ 0 y_i > U_i \end{cases} \tag{4}$$

where U_i and L_i represents the upper and lower limits for the response, respectively. The parameter r determines the importance of the output response to be close to the desired value. In this study, a value of 1 has been assigned to r for all responses, indicating the adoption of a linear function to determine the desirability of the responses [41]. The overall desirability (D) can be calculated as follows:

$$D = \left(\prod_{i=1}^{n} d_i\right)^{\frac{1}{n}} \tag{5}$$

where n is the number of responses. In this study, the utilization of Design-Expert software facilitates the optimization of the investigated responses. Additionally, it is notable that equal weight is allocated to all responses.

3. Results and discussion

The RSM is a mathematical and statistical method for modeling the relation between the input variables, including interactions, and the annual energy output and LCOE of a CSP plant. The RSM enables the evaluation of each control factor independently and determines the best configurations for independent parameters that maximize annual energy output while lowering the LCOE. Furthermore, based on input variables and their interactions, the RSM can develop a regression model that represents the annual energy generation and the LCOE of a proposed CSP system design.

3.1. Predictive models

A regression model is constructed using the data in Table 5, to define annual energy production in kWh and LCOE in (¢/kWh) relative to solar multiple (A), row spacing (B), number of assemblies per loop (C), thermal energy storage size (D), and their interactions are formulated in Equations (3) and (4).

$$\begin{aligned} Energy(kWh) = {} & (-710.27 + 1077.82A + 21.15B + 30.24C + 60.41D \\ & - 0.78AB + 8.45AC + 29.85AD + 0.74BC - 0.25BD \\ & + 0.48CD - 153.57A^2 - 0.48B^2 - 5.25C^2 - 4.54D^2) \\ & \times 10^5 \end{aligned} \tag{6}$$

Table 6
Comparison of the different cooling methods considering energy and LCOE optimization.

Optimization		Solar multiple	Row spacing (m)	No. of assemblies per loop	Thermal energy storage size (h)	Energy (kWh)	Capacity factor (%)	LCOE (¢/kWh)	Water consumption (m^3)	Area (Acres)
Energy	LCOE									
Air										
Maximize	×	4.94935	23.6839	9	14.9707	343,032,000	78.3468	19.4001	97593.3	2128.24
×	Minimize	3.20997	23.3178	5	8.39963	252,548,000	57.6977	19.0042	66203.1	1360.73
Maximize	Minimize	4.94431	18.1789	7	14.9874	341,237,000	77.933	19.2392	96907.1	1630.09
Evaporative										
Maximize	×	4.99112	14.2096	8	14.9966	341,537,000	78.0168	19.5984	1.27×10^6	1286.18
×	Minimize	3	20	6	10	257,565,000	58.8246	19.4703	945,780	1091.28
Maximize	Minimize	4.9314	14.4766	8	14.9947	341,375,000	77.9799	19.4856	1.269×10^6	1294.8
Hybrid										
Maximize	×	4.93638	19.3571	10	14.812	344,247,000	78.5683	19.5599	687,079	1736.65
×	Minimize	4.55556	18.6667	7	11.1111	310,263,000	70.8601	18.9583	615,404	1543.9
Maximize	Minimize	4.99939	16.6131	7	14.9997	344,161,000	78.5782	19.3108	680,023	1506.03

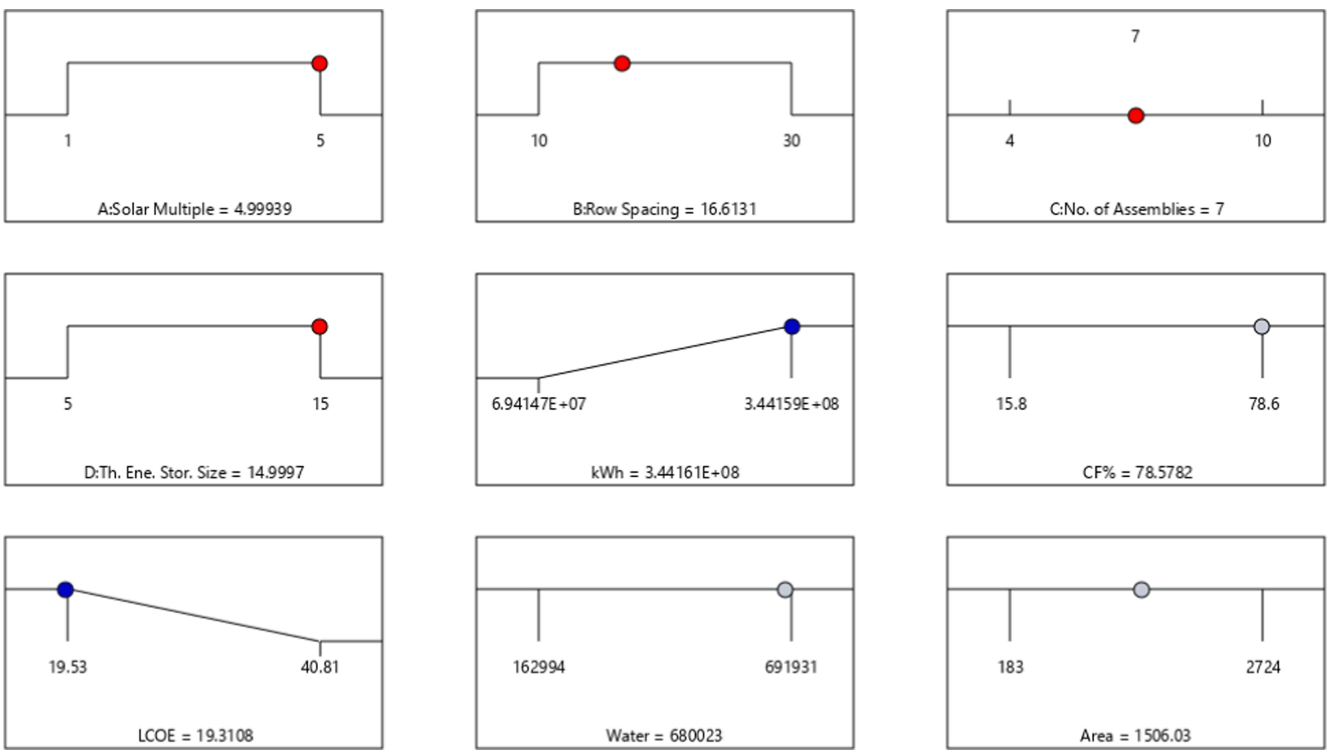

Fig. 4. Energy and LCOE optimization for the hybrid cooling system.

$$
\begin{aligned}
LCOE(¢/kWh) = {} & 36.13 - 8.17A - 0.25B - 0.27C + 0.37D + 0.03AB \\
& - 0.13AC - 0.33AD - 0.01BC - 0.002BD + 0.01CD \\
& + 1.55A^2 + 0.01B^2 + 0.06C^2 + 0.04D^2
\end{aligned} \tag{7}
$$

To derive Equations (3) and (4), it is necessary to carry out 30 experimental trials with different input factors, as shown in Table 5. The annual energy for each trial is then estimated using SAM, and regression modeling is conducted utilizing Design-Expert software. After that, the data is fitted to a general second-order polynomial model (Equation (2). The ordinary least squares method is used in this equation to find the model's coefficients (β values), with the aim of minimizing the sum of squared errors between the predicted and observed responses. This approach optimally adjusts the β values to ensure that the aggregate of these squared errors is as small as possible, enhancing the model's predictive accuracy. The obtained coefficient of determination (R2) of 0.99 highlights both models' high accuracy and reliability in predicting annual energy production and LCOE within the designated parameter range. The efficiency of the proposed mathematical model is further demonstrated in Fig. 2, which compares the energy output and LCOE results obtained by SAM with estimated outcomes from Design-Expert. This comparison reveals a significant agreement between the projected and simulated values of both the annual energy and LCOE, thus confirming the reliability of the predictive models.

3.2. *Responses optimization*

In this section, multiple optimization steps are undertaken, beginning with the selection of the optimal cooling system. Then, the required area is optimized using the chosen cooling system. Following this, an investigation is conducted into the effect of varying areas on both the energy output and LCOE of the CSP plant. The analysis is performed at area sizes surrounding the determined optimal value.

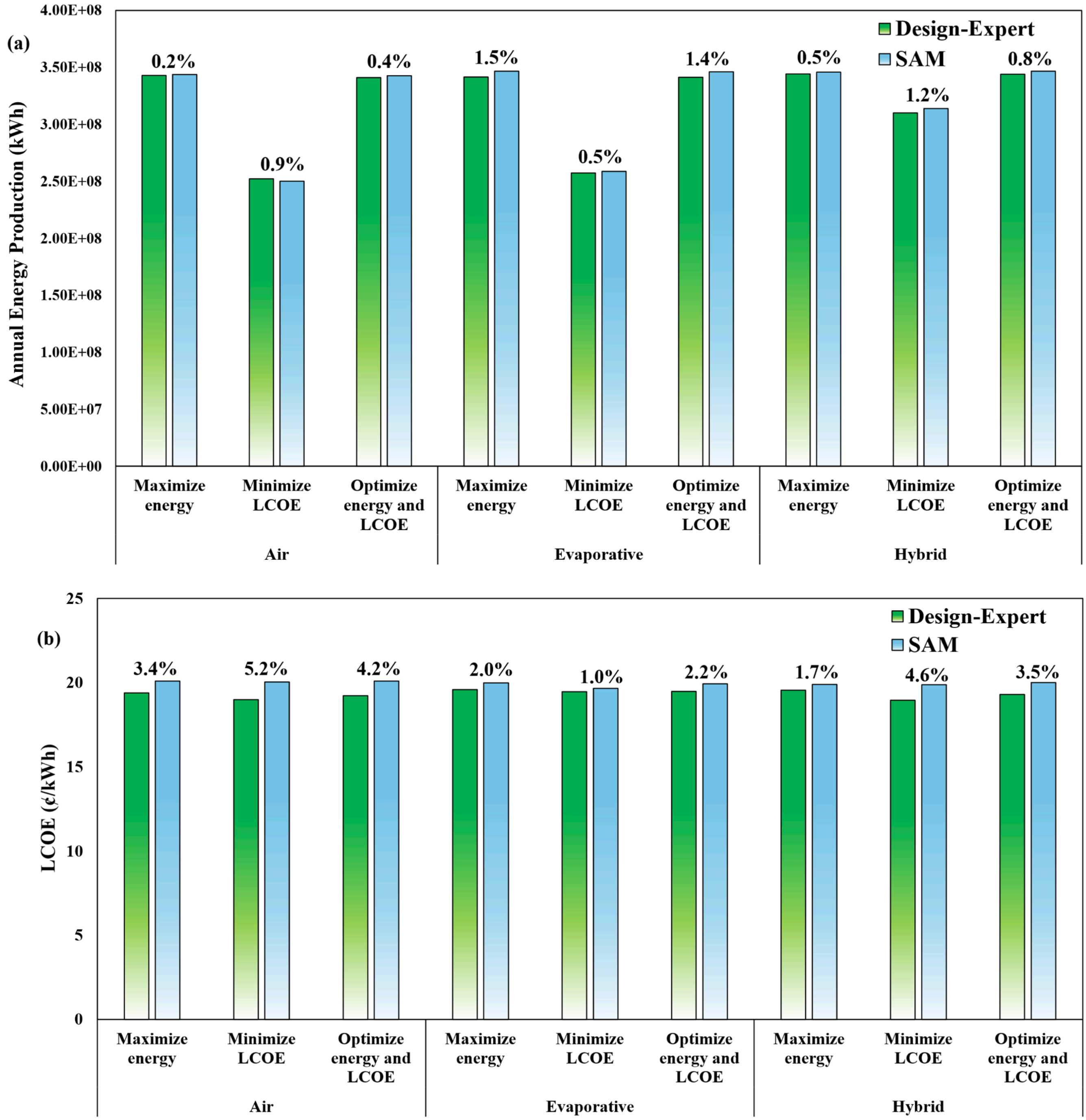

Fig. 5. Validation results for the (a) annual energy production and (b) LCOE for the air, evaporative, and hybrid cooling techniques. The percentages represent the errors.

3.2.1. Cooling techniques comparison

A comparison of the different cooling techniques (air, evaporative, and hybrid) is carried out while optimizing energy and LCOE. A schematic diagram of the investigated CSP system is presented in Fig. 3 demonstrating the difference between the cooling techniques configurations.

All results are summarized in Table 6, showing the differences between the three systems in terms of designs and responses. Among the different optimization approaches, the multi-objective optimization stands as the best approach for all cooling techniques, as it presents almost similar values of energy compared to the case of maximizing energy alone and an average LCOE of the other single-objective approaches. The worst scenario can be referred to the LCOE minimization, which led to a massive decrease in energy production. As an example, the energy output decreases from 3.41 $\times$ 10^8 to 2.52 $\times$ 10^8 kWh in the air-cooling method and from 3.41 $\times$ 10^8 to 2.57 $\times$ 10^8 for the evaporative cooling technique while minimizing the LCOE, compared to the multi-objective approach. However, this reduction is not as pronounced in the case of hybrid cooling where the energy decreased only from 3.44 $\times$ 10^8 to 3.10 $\times$ 10^8 kWh. Among the different cooling methods, the hybrid technique demonstrates the best option since it achieves the highest energy production with a value of 3.44 $\times$ 10^8 kWh and an acceptable LCOE of 19.31 ¢/kWh which is less than that of the evaporative (19.49 ¢/kWh) and slightly higher than that of air (19.24 ¢/kWh) when considering the multi-objective optimization. This case, which is related to energy maximization and LCOE minimization for the hybrid

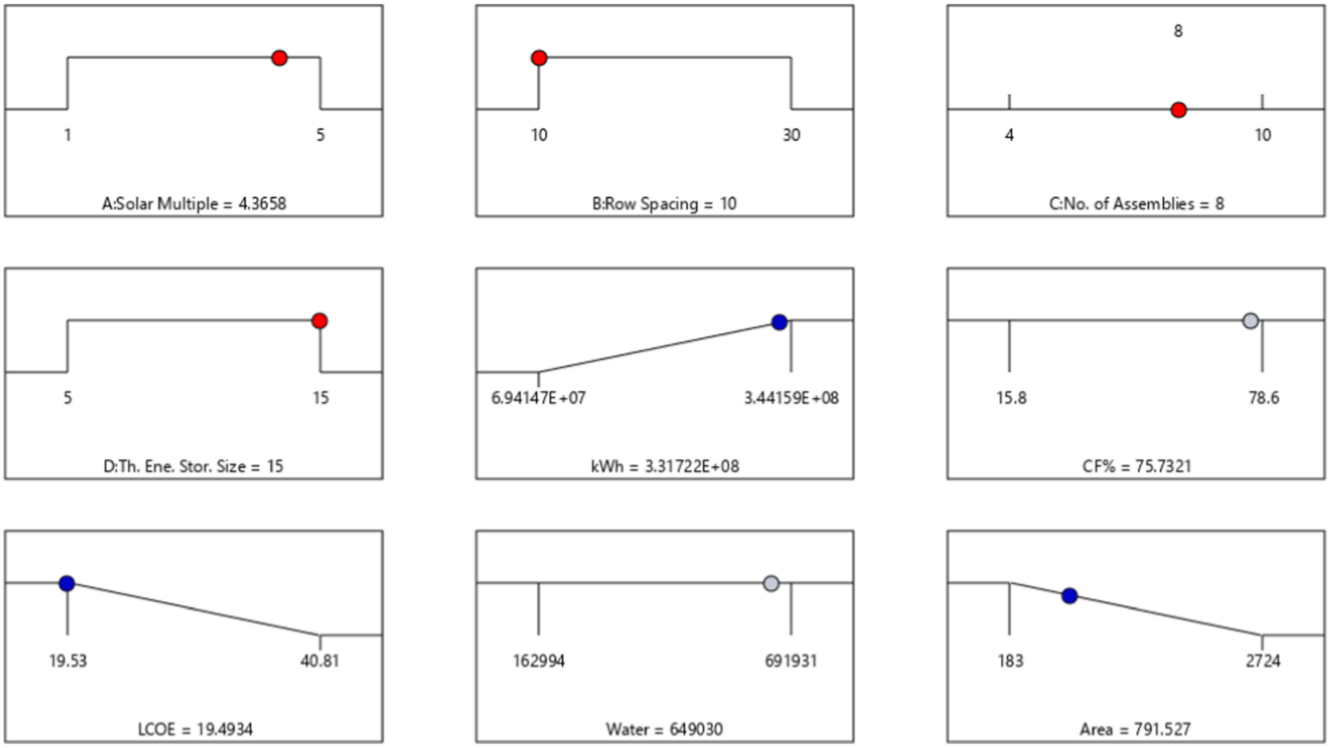

Fig. 6. Energy and LCOE optimization with area minimization for the hybrid cooling system.

Table 7
Effect of area on energy generation and LCOE.

Parameter					Responses		SAM		Error	
Area (Acres)	A	B	C	D	Energy (kWh) x10^8	LCOE (¢/kWh)	Energy (kWh) x10^8	LCOE (¢/kWh)	Energy Error	LCOE Error
350	1.90	10.13	6	8.90	1.75	24.51	1.65	22.82	−6.06	−7.40
500	2.72	10.11	5	12.60	2.46	22.10	2.37	20.88	−3.80	−5.84
650	3.53	10.13	6	13.07	2.93	19.74	2.89	19.78	−1.38	0.20
791.5	4.37	10	8	15	3.32	19.49	3.27	19.79	−1.53	1.52
1300	4.75	15.06	10	14.37	3.37	19.59	3.42	19.65	1.46	0.31
1800	4.87	20.36	9	14.25	3.40	19.20	3.45	19.78	1.45	2.93
2300	4.76	26.60	10	14.96	3.43	19.36	3.42	19.93	−0.29	2.86

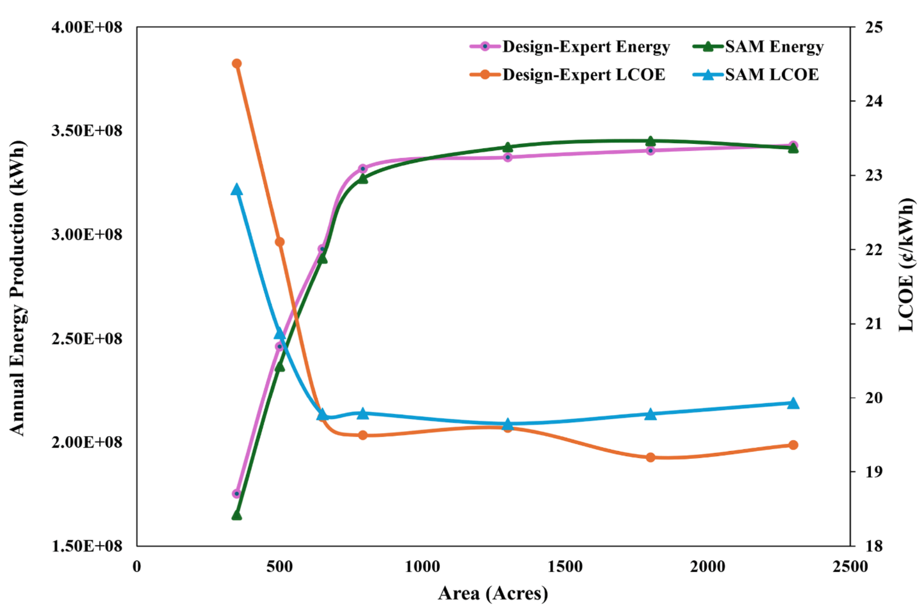

Fig. 7. Comparison of SAM and Design-Expert models under specific values of area.

Table 8
ANOVA for energy production and LCOE.

Source	Energy (p-value)	Significant	LCOE (p–value)	Significant
A	< 0.0001	✔	< 0.0001	✔
B	0.0815		0.0175	✔
C	0.6876		0.0205	✔
D	< 0.0001	✔	< 0.0001	✔
AB	0.2753		0.0066	✔
AC	0.0022	✔	0.0005	✔
AD	< 0.0001	✔	< 0.0001	✔
BC	0.1265		0.1345	
BD	0.3742		0.5857	
CD	0.6050		0.3149	
A^2	< 0.0001	✔	< 0.0001	✔
B^2	0.1826		0.2213	
C^2	0.1865		0.2132	
D^2	0.0046	✔	0.0298	✔

method, is depicted in Fig. 4, extracted from the Design-Expert software, where the red dots represent the optimal values of the investigated input factors, the blue dots indicate the corresponding responses to be optimized (energy and LCOE), and the grey dots indicate the responses that are not optimized. Although the hybrid method presented the best option, it is worth noting that investigating the two other methods is essential since, under certain circumstances, employing one of them could be necessary, such as in regions where there is an insufficient amount of water. In such cases, the air-cooled method would be the only system that can be used. However, if the cooling method is changed, it is also necessary to modify the design as well, which is clear from the results presented in Table 6. For example, the row spacing in the case of multi-objective optimization for air, evaporative, and hybrid-cooled is 18.2, 14.5, and 16.6 m, respectively.

In a real application, the balance between LCOE and energy is directly related to the scale of the power plant and land availability/cost. For example, if there is a huge land available, then it would be recommended to optimize the system based on energy maximization only. However, if a small land area is available, then minimizing the LCOE will be the main target. From this perspective, land availability/cost is the most effective factor that controls the weight of these two key performance indices, which is discussed in detail in the next section.

Optimizing the energy and LCOE of CSP plants can significantly

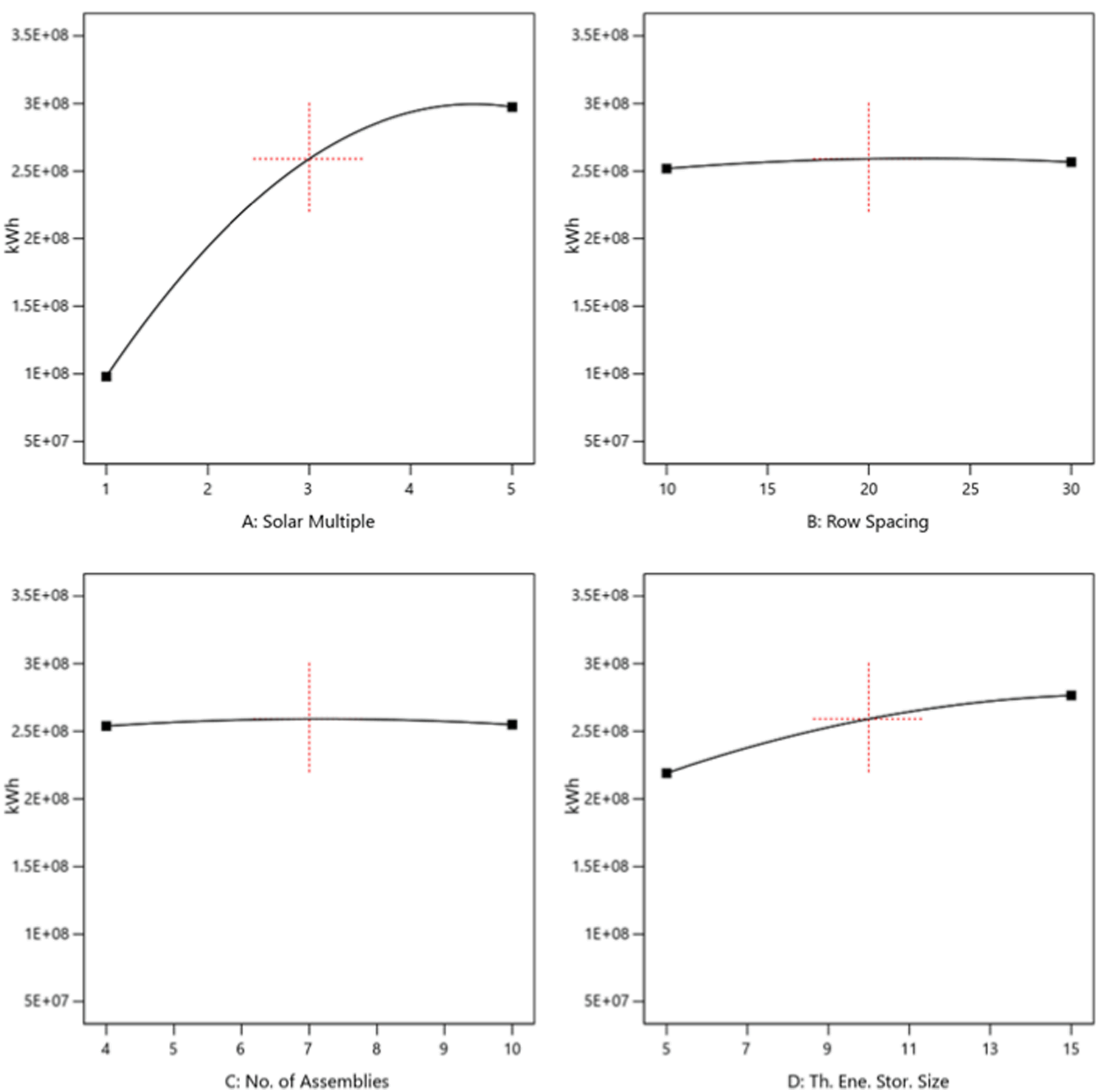

Fig. 8. The main effects of (A) solar multiple, (B) row spacing, (C) number of assemblies, and (D) thermal energy storage size on the annual energy produced.

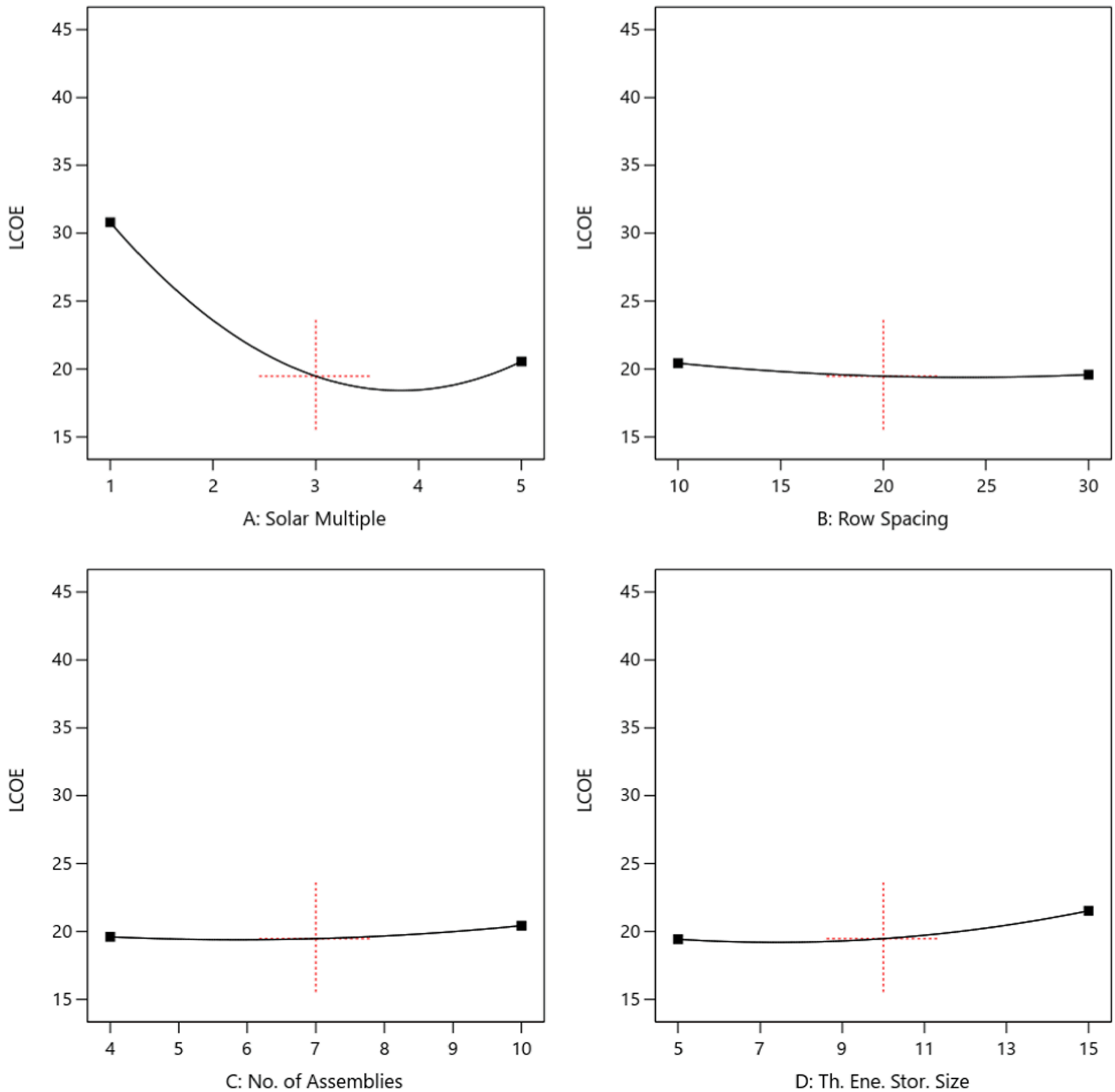

Fig. 9. The main effects of (A) solar multiple, (B) row spacing, (C) number of assemblies, and (D) thermal energy storage size on the levelized cost of electricity.

enhance the contribution to decarbonization and climate change mitigation, as it reduces reliance on fossil fuels, cutting greenhouse gas emissions. By decreasing the LCOE of CSP plants, they become more economically viable, encouraging wider adoption and investment. Such optimizations directly align with several United Nations Sustainable Development Goals (SDGs), fostering a holistic approach to sustainability. By improving energy efficiency and reducing costs, optimized CSP plants contribute to SDG 7, which aims to ensure access to affordable and clean energy. The reduction in greenhouse gas emissions supports SDG 13, which focuses on taking urgent action to combat climate change and its impacts. Furthermore, the cost savings of optimized CSP plants can stimulate economic growth in the renewable energy sector, advancing SDG 8.

The values of the annual energy and LCOE for the nine scenarios in Table 6 are validated using the SAM model and the results showed high accuracy of the predictive models, as depicted in Fig. 5. The diversity in verification procedures encompassing nine runs proves the robustness of the predictive models. This is clearer in the case of energy evaluation since the error did not exceed 1.5 % (see Fig. 5a). However, the error in the case of LCOE is slightly higher, but still acceptable, ranging from 1 % to 5.2 % (see Fig. 5b). These findings verify that the generated predictive model can be used as a reliable tool for estimating the responses in CSP applications under the investigated factors' range. Additionally, there is an inconsiderable difference between the errors of the cooling techniques.

3.2.2. *Optimization of land area*

Effective land use is critical to conservation efforts, particularly when it comes to the infrastructure of power plants. Attaining this equilibrium between conservation of land and efficiency enhancement is essential. In addition to the relationship between the SDGs and the optimization of energy and cost, land use optimization is also linked to these goals, promoting a balanced and sustainable approach to land management that benefits both people and the planet. By efficiently using land resources, land use optimization mainly supports SDG 15, which aims to protect, restore, and promote sustainable use of terrestrial ecosystems, manage forests sustainably, combat desertification, and halt and reverse land degradation and biodiversity loss. By optimizing the land area of CSP plants, it is possible to maximize solar energy capture while minimizing environmental impact. Efficient land use also means

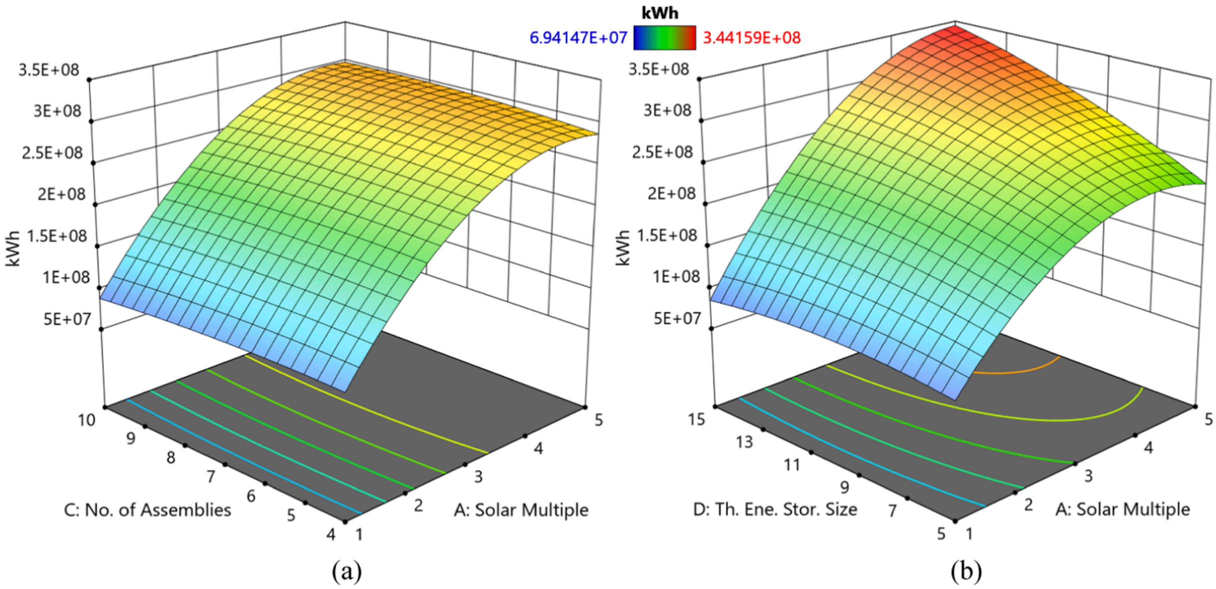

Fig. 10. Energy interaction effects; (a) A and C, (b) A and D.

integrating CSP with other land uses, such as agriculture, which allows for dual use of land and enhances land productivity. By reducing land competition and optimizing land resources, CSP plants can generate more clean energy with lower carbon footprints, directly reducing greenhouse gas emissions. This contributes to the broader decarbonization goals by displacing fossil fuel-based power generation and supporting a sustainable transition to renewable energy sources, ultimately aiding in the global effort to combat climate change, which agrees with SDG 13.

In this study, the Design-Expert software is used to provide the best design parameters, as illustrated in Fig. 6, which also shows the expected performance metrics, where the red dots represent the optimal values of the investigated input factors, the blue dots indicate the corresponding responses to be optimized (energy, LCOE, and area), and the grey dots indicate the responses that are not optimized. When comparing the obtained findings to the optimization scenario that specifically considers energy and LCOE in the hybrid cooling system, as shown in Fig. 4, a slight difference in performance is observed although the area declined from 1506.03 to 791.53 acres. More precisely, there is a negligible drop in energy production of 3.61 % and a small rise in LCOE by 0.95 %. Significantly, there is a considerable decrease in the needed area by 47.44 %. The validation of these findings is conducted using SAM, resulting in an energy production of 3.27×10^8 kWh and an LCOE of 19.79 ¢/kWh. The validation process demonstrated a minimal margin of error of 1.44 % for energy and 1.5 % for LCOE, highlighting the high level of precision of the obtained outcomes.

3.2.3. Investigating the effect of the area on energy and levelized cost of electricity

In this section, simulations are carried out in multiple areas to evaluate the impact of the area on the performance of the power plant. Upon examination of the outcomes derived from the SAM as depicted in a matrix table, a diverse array of appropriate regions ranging from 183 to 2724 acres is identified. Based upon the previous section in which a total size of 791.5 acres is identified as the most favorable, we have chosen six specific area values, three exceeding and three falling below this threshold (=791.5), within the designated range, for further examination.

The results derived using Design-Expert are verified using SAM and are presented in Table 7 and Fig. 7. It is important to note that a significant rise in the LCOE is observed when operating within the three constrained areas measuring less than 650 acres. On the other hand, expanding the area beyond this threshold does not result in significant changes.

Moreover, when the area falls below the optimal threshold of 791.5 acres, there is an obvious decrease in energy production. However, there are slight advantages to be gained by increasing the size of the area, as illustrated in Fig. 7. When examining the scenario of 791.5 acres as a reference point, it is observed that the energy output experiences a maximum rise of 3.36 % when utilizing 2300 acres with a reduction of 0.68 % in the LCOE, leading to a significant land-saving of about 190.58 %. In contrast, decreasing the size of the area has a substantial effect on performance measures, resulting in a maximum loss in energy of 47.2 % and a corresponding increase of 25.76 % in LCOE. The results mentioned above highlight the significant importance of area optimization in ensuring the effective functioning of the CSP plant.

3.3. Statistical analysis

In this section, statistical analysis is carried out utilizing Design-Expert software to investigate and optimize simulation conditions. The statistical significance of the model and its parameters is assessed using Analysis of Variance (ANOVA). Both the main effects, which demonstrate the influence of individual factors on the response variable, and the interaction effects, which illustrate how multiple factors interact to affect the outcome, are analyzed. The use of these statistical methods facilitated a complete understanding of the factors affecting the system and aided in the determination of the most beneficial conditions for improved performance.

3.3.1. Analysis of variance

The Analysis of Variance (ANOVA) serves as a frequently utilized statistical method for assessing the influence of input variables and their interactions on a response variable, such as annual energy generation and LCOE. In this study, ANOVA is utilized with a significance level (SL) set at 5 %. The determination of the P-value for each factor acts as an indicator of its statistical significance. Typically, factors with P-values below the SL threshold are considered statistically significant. It is important to note that six effects (A, D, A^2, D^2, AC, and AD) demonstrate P-values that are less than 0.05 for the energy output and nine effects (A, B, C, D, A^2, D^2, AB, AC, and AD) for the LCOE, the data demonstrates statistical significance with a confidence level of 95 %. Table 8 emphasizes these effects.

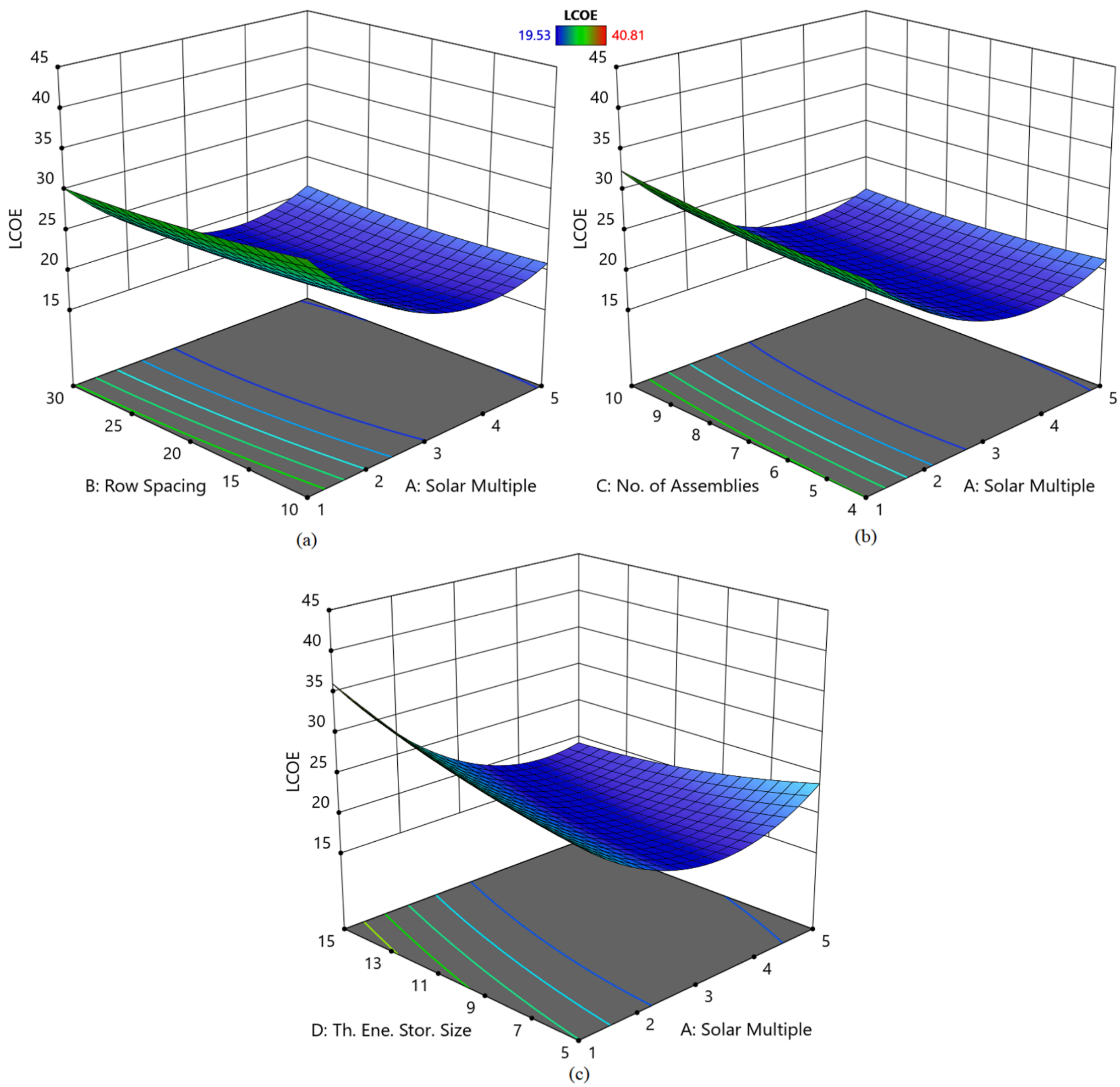

Fig. 11. LCOE interaction effects; (a) A and B, (b) A and C, (c) A and D.

3.3.2. *Main effect*

The main effect plots, shown in Fig. 8 and Fig. 9, are the key tools used to estimate the significant variables that affect the annual energy output and LCOE of the CSP plant model. Solar multiple and thermal energy storage size are considered statistically significant parameters when there is a significant difference in response values between low and high levels. This plot facilitates the identification of the most favorable levels for these critical factors in order to accomplish the goals of maximizing yearly energy production and decreasing the LCOE. As shown in Fig. 8A and Fig. 9A, increasing the solar multiple enhances the annual output of energy while decreasing the LCOE. The reason for this is that a greater solar multiple means a larger solar field to run the power block, leading to an increase in energy output and a decrease in the LCOE. However, exceeding a specific threshold can result in an excessively large solar field, which has the potential to reduce efficiency. Similarly, increasing the size of the thermal energy storage improves energy production and decreases the LCOE, as presented in Fig. 8D and Fig. 9D, respectively. However, excessive sizing might result in inefficiencies, necessitating extra energy to prevent the heat transfer fluid from freezing. Insufficient energy storage may occur when storage is small, particularly during periods of strong solar irradiation. The major benefit of the main effect plot is to provide a graphical representation of the impact of different factor levels on responses, revealing the extent and direction of these effects. The RSM is known for its ability to consider nonlinear interactions between factors and responses, distinguishing it from other experimental design methods such as factorial design. For example, it is expected that row spacing adjustments result in a nonlinear increase. However, modifying the solar multiple leads to a nonlinear decrease in response, which is also observed in the size of TES. Notably, neither row spacing nor the number of assemblies per loop has significant effects on the responses, which is clear from Fig. 8B, Fig. 8C, Fig. 9B, and Fig. 9C.

3.3.3. *Interaction effect*

Surface plots depicting important interactions are presented in Fig. 10 and Fig. 11. Surface plots are highly helpful tools for accurately determining the appropriate response values within certain operational parameters. Surface plots, commonly illustrated in a three-dimensional format, provide a more accurate depiction of the response, hence enabling a better comprehension of the interplay among various elements. Fig. 10b illustrates the annual variation in the system's energy output based on the solar multiple and the size of TES. Maximizing annual energy generation can be achieved by raising the size of the TES while simultaneously raising the solar multiple to its maximum value. Fig. 11c shows that increasing the size of the TES to its maximum (15 h) within the solar multiple range of 3 to 5 results in a decrease in the LCOE, indicating a perfect configuration for cost efficiency.

4. Conclusions

In this study, a combination of SAM and Design-Expert software is utilized to validate and demonstrate the influence of several parameters and their interactions on the annual energy production and LCOE of a CSP plant. The impact of solar multiple (A), row spacing (B), number of assemblies per loop (C), and thermal energy storage size (D) is investigated utilizing parabolic trough collectors and different cooling methods (evaporative, air, and hybrid cooling). The corresponding ranges for the studied parameters are considered as 1–5, 10–30 m, 4–10, and 5–15 h, respectively. The process of modeling and validation is conducted in order to compare and validate the model accurately with the actual data acquired from the power plant. Then, the RSM is utilized to enhance the system's annual energy production and LCOE. The following can be concluded:

1. The hybrid cooling system in CSP plants showed great potential in providing higher energy production efficiency and lower LCOE compared to the conventional evaporative and air-cooling systems while also reducing the huge amounts of water required in the evaporative cooling method.
2. Under the investigated ranges, the generated predictive model of the annual energy production exhibited high precision with an error ranging between 0.2 % and 1.5 %. Additionally, the predictive model of the LCOE is also accurate but with a slightly higher error, ranging from 1.0 % to 5.2 %.
3. Reducing the required area of the power plant is an essential consideration to minimize the capital cost. When optimizing the area of the power plant (saving around 47.44 %), energy production decreased by 3.61 %, while the LCOE slightly increased by 0.95 %.
4. When examining multiple areas, the performance can vary significantly, especially if it falls below the optimal value. This can lead to a significant decrease in energy production and an increase in the LCOE. However, in areas above the optimal value, this effect becomes insignificant and energy production does not experience a significant increase, while the LCOE starts to slightly increase.
5. Based on the ANOVA, it has been found that there are six parameters (A, D, A^2, D^2, AC, and AD) that affect the energy output and nine parameters (A, B, C, D, A^2, D^2, AB, AC, and AD) that affect the LCOE.
6. Further investigations are needed to consider more parameters in the design as well as to consider other CSP plant designs including (solar tower and linear Fresnel).

The proposed approach has great potential to optimize CSP plants; however, it is limited to the investigated input factors' ranges. In addition, it is not beneficial to extensively expand these ranges because this may decrease the accuracy of the predictive models. Future studies could focus on a detailed analysis of the economic and environmental impacts of CSP plants considering different ranges for the investigated factors. This would involve a comprehensive cost-benefit analysis, including life-cycle assessments and the potential for carbon footprint reduction. It is also worthwhile expanding the study to include CSP plants in different geographical locations and under various climatic conditions, which would help generalize the findings. This would involve collecting and analyzing data from a wider range of sites.

CRediT authorship contribution statement

Ayman Mdallal: Writing – review & editing, Writing – original draft, Methodology, Formal analysis, Data curation. **Salah Haridy:** Writing – review & editing, Writing – original draft, Software, Methodology, Formal analysis. **Montaser Mahmoud:** Writing – review & editing, Writing – original draft, Methodology, Formal analysis, Data curation. **Abdul Hai Alami:** Writing – review & editing, Writing – original draft, Validation, Methodology, Investigation. **Abdul Ghani Olabi:** Writing – review & editing, Writing – original draft, Validation, Supervision. **Mohammad Ali Abdelkareem:** Writing – review & editing, Writing – original draft, Supervision, Conceptualization.

Declaration of competing interest

The authors declare that they have no known competing financial interests or personal relationships that could have appeared to influence the work reported in this paper.

Data availability

No data was used for the research described in the article.

References

[1] El Marazgioui S, El Fadar A. Impact of cooling tower technology on performance and cost-effectiveness of CSP plants. Energy Convers Manag Apr. 2022;258:115448. https://doi.org/10.1016/J.ENCONMAN.2022.115448.

[2] Abdel-Basset M, El-Shahat D, Chakrabortty RK, Ryan M. Parameter estimation of photovoltaic models using an improved marine predators algorithm. Energy Convers Manag Jan. 2021;227:113491. https://doi.org/10.1016/J.ENCONMAN.2020.113491.

[3] "Executive summary – Electricity 2024 – Analysis - IEA." Accessed: May 23, 2024. [Online]. Available: https://www.iea.org/reports/electricity-2024/executive-summary.

[4] "Renewable capacity statistics 2024." Accessed: May 23, 2024. [Online]. Available: https://www.irena.org/Publications/2024/Mar/Renewable-capacity-statistics-2024.

[5] Aboelmaaref MM, et al. Hybrid solar desalination systems driven by parabolic trough and parabolic dish CSP technologies: Technology categorization, thermodynamic performance and economical assessment. Energy Convers Manag Sep. 2020;220:113103. https://doi.org/10.1016/J.ENCONMAN.2020.113103.

[6] Allouhi H, Allouhi A, Jamil A. Multi-objective optimization of a CSP-based dish Stirling field layout using Genetic Algorithm and TOPSIS method: Case studies in Ouarzazate and Madrid. Energy Convers Manag Feb. 2022;254:115220. https://doi.org/10.1016/J.ENCONMAN.2022.115220.

[7] Baghaei Oskouei S, et al. Solar-powered hybrid energy storage system with phase change materials. Energy Convers Manag Feb. 2024;302:118117. https://doi.org/10.1016/J.ENCONMAN.2024.118117.

[8] Abraim M, et al. Techno-economic assessment of soiling losses in CSP and PV solar power plants: A case study for the semi-arid climate of Morocco. Energy Convers Manag Oct. 2022;270:116285. https://doi.org/10.1016/J.ENCONMAN.2022.116285.

[9] Alami AH, et al. Concentrating solar power (CSP) technologies: Status and analysis. International Journal of Thermofluids May 2023;18:100340. https://doi.org/10.1016/J.IJFT.2023.100340.

[10] "Concentrating Solar Power Projects by Status | Concentrating Solar Power Projects | NREL." Accessed: Feb. 28, 2024. [Online]. Available: https://solarpaces.nrel.gov/by-status.

[11] F. M. Aprà, S. Smit, R. Sterling, and T. Loureiro, "Overview of the Enablers and Barriers for a Wider Deployment of CSP Tower Technology in Europe," *Clean Technologies 2021, Vol. 3, Pages 377-394*, vol. 3, no. 2, pp. 377–394, Apr. 2021, doi: 10.3390/CLEANTECHNOL3020021.

[12] Liqreina A, Qoaider L. Dry cooling of concentrating solar power (CSP) plants, an economic competitive option for the desert regions of the MENA region. Sol Energy May 2014;103:417–24. https://doi.org/10.1016/J.SOLENER.2014.02.039.

[13] Zayed ME, Zhao J, Elsheikh AH, Li W, Elaziz MA. Optimal design parameters and performance optimization of thermodynamically balanced dish/Stirling concentrated solar power system using multi-objective particle swarm optimization. Appl Therm Eng Sep. 2020;178:115539. https://doi.org/10.1016/J.APPLTHERMALENG.2020.115539.

[14] Li X, et al. Operation optimization of electrical-heating integrated energy system based on concentrating solar power plant hybridized with combined heat and power plant. J Clean Prod Mar. 2021;289:125712. https://doi.org/10.1016/J.JCLEPRO.2020.125712.

[15] Jiang P, Dong J, Huang H. Optimal integrated demand response scheduling in regional integrated energy system with concentrating solar power. Appl Therm Eng Feb. 2020;166:114754. https://doi.org/10.1016/J.APPLTHERMALENG.2019.114754.

[16] Hamilton WT, Husted MA, Newman AM, Braun RJ, Wagner MJ. Dispatch optimization of concentrating solar power with utility-scale photovoltaics. Optim Eng Mar. 2020;21(1):335–69. https://doi.org/10.1007/S11081-019-09449-Y/METRICS.

[17] Elbeh MB, Sleiti AK. Analysis and optimization of concentrated solar power plant for application in arid climate. Energy Sci Eng Jun. 2021;9(6):784–97. https://doi.org/10.1002/ESE3.742.

[18] Ma Y, Morosuk T, Luo J, Liu M, Liu J. Superstructure design and optimization on supercritical carbon dioxide cycle for application in concentrated solar power plant. Energy Convers Manag Feb. 2020;206:112290. https://doi.org/10.1016/J.ENCONMAN.2019.112290.

[19] Liang Y, Chen J, Luo X, Chen J, Yang Z, Chen Y. Simultaneous optimization of combined supercritical CO2 Brayton cycle and organic Rankine cycle integrated with concentrated solar power system. J Clean Prod Sep. 2020;266:121927. https://doi.org/10.1016/J.JCLEPRO.2020.121927.

[20] Trevisan S, Guédez R, Laumert B. Thermo-economic optimization of an air driven supercritical CO2 Brayton power cycle for concentrating solar power plant with packed bed thermal energy storage. Sol Energy Nov. 2020;211:1373–91. https://doi.org/10.1016/J.SOLENER.2020.10.069.

[21] Ahmad M, Zeeshan M. Multi-objective optimization of concentrated solar power plants from an energy-water-environment nexus perspective under distinct climatic conditions – Part B: Environ-economic analysis. J Clean Prod Jan. 2023;385:135689. https://doi.org/10.1016/j.jclepro.2022.135689.

[22] Cox JL, Hamilton WT, Newman AM, Wagner MJ, Zolan AJ. Real-time dispatch optimization for concentrating solar power with thermal energy storage. Optim Eng Jun. 2023;24(2):847–84. https://doi.org/10.1007/S11081-022-09711-W/METRICS.

[23] Wang P, Hu B, Tai N, Zhao L, Vafai K. Peak shaving auxiliary service analysis for the photovoltaic and concentrating solar power hybrid system under the planning-dispatch optimization framework. Energy Convers Manag Nov. 2023;295:117609. https://doi.org/10.1016/J.ENCONMAN.2023.117609.

[24] Berger PD, Maurer RE, Celli GB. Introduction to Response-Surface Methodology. Exp Des 2018:533–84. https://doi.org/10.1007/978-3-319-64583-4_16.

[25] K. Palanikumar and K. Palanikumar, "Introductory Chapter: Response Surface Methodology in Engineering Science," *Response Surface Methodology in Engineering Science*, Nov. 2021, doi: 10.5772/INTECHOPEN.100484.

[26] Kumar R, Reji M. Response surface methodology (RSM): An overview to analyze multivariate data. Indian J Microbiol Res Jan. 2023;9(4):241–8. https://doi.org/10.18231/J.IJMR.2022.042.

[27] Assareh E, Mousavi Asl SS, Ahmadinejad M, Parvaz M, Ghodrat M. Optimization of a solar energy system integrating cooling, hot water, and power units in Australian cities: A climate-based analysis and cost-efficiency investigation. Int J Hydrogen Energy Jan. 2024;49:353–75. https://doi.org/10.1016/J.IJHYDENE.2023.08.035.

[28] Rejeb O, Shittu S, Ghenai C, Li G, Zhao X, Bettayeb M. Optimization and performance analysis of a solar concentrated photovoltaic-thermoelectric (CPV-TE) hybrid system. Renew Energy Jun. 2020;152:1342–53. https://doi.org/10.1016/J.RENENE.2020.02.007.

[29] Radwan A, Mdallal A, Haridy S, Abdelkareem MA, Alami AH, Olabi AG. Optimizing the annual energy yield of a residential bifacial photovoltaic system using response surface methodology. Renew Energy Feb. 2024;222:119914. https://doi.org/10.1016/j.renene.2023.119914.

[30] "Home - System Advisor Model - SAM." Accessed: May 23, 2024. [Online]. Available: https://sam.nrel.gov/.

[31] "Design-Expert | Stat-Ease." Accessed: May 23, 2024. [Online]. Available: https://www.statease.com/software/design-expert/.

[32] "The parabolic trough power plants Andasol 1 to 3 The largest solar power plants in the world-Technology premiere in Europe".

[33] "NSRDB." Accessed: May 23, 2024. [Online]. Available: https://nsrdb.nrel.gov/data-viewer.

[34] Andasol-, "System Advisor Model (SAM) Case Study".

[35] Chen WH, et al. A comprehensive review of thermoelectric generation optimization by statistical approach: Taguchi method, analysis of variance (ANOVA), and response surface methodology (RSM). Renew Sustain Energy Rev Nov. 2022;169:112917. https://doi.org/10.1016/J.RSER.2022.112917.

[36] Khuri AI, Mukhopadhyay S. Response surface methodology. Wiley Interdiscip Rev Comput Stat Mar. 2010;2(2):128–49. https://doi.org/10.1002/WICS.73.

[37] Sarabia LA, Ortiz MC. Response Surface Methodology. Comprehensive Chemometrics Jan. 2009;1:345–90. https://doi.org/10.1016/B978-044452701-1.00083-1.

[38] Ferreira SLC, et al. Statistical designs and response surface techniques for the optimization of chromatographic systems. J Chromatogr A Jul. 2007;1158(1–2):2–14. https://doi.org/10.1016/J.CHROMA.2007.03.051.

[39] Kazemian A, Khatibi M, Reza Maadi S, Ma T. Performance optimization of a nanofluid-based photovoltaic thermal system integrated with nano-enhanced phase change material. Appl Energy Aug. 2021;295:116859. https://doi.org/10.1016/J.APENERGY.2021.116859.

[40] Derringer G, Suich R. Simultaneous Optimization of Several Response Variables. J Qual Technol Oct. 1980;12(4):214–9. https://doi.org/10.1080/00224065.1980.11980968.

[41] I. Buj-Corral, A. Bagheri, and M. Sivatte-Adroer, "Effect of Printing Parameters on Dimensional Error, Surface Roughness and Porosity of FFF Printed Parts with Grid Structure," *Polymers 2021, Vol. 13, Page 1213*, vol. 13, no. 8, p. 1213, Apr. 2021, doi: 10.3390/POLYM13081213.